J|A|C|S
ARTICLES
Published on Web 02/27/2002

EXHIBIT A

The Interaction of MS-325 with Human Serum Albumin and Its Effect on Proton Relaxation Rates

Peter Caravan,*,† Normand J. Cloutier,† Matthew T. Greenfield,† Sarah A. McDermid,† Stephen U. Dunham,† Jeff W. M. Bulte,† John C. Amedio, Jr.,† Richard J. Looby,† Ronald M. Supkowski,§ William DeW. Horrocks, Jr.,§ Thomas J. McMurry,† and Randall B. Lauffer†

Contribution from EPIX Medical, Inc., 71 Rogers Street, Cambridge, Massachusetts 02142-1118, Laboratory of Diagnostic Radiology Research (CC), National Institutes of Health, BLDG 10, Room B1N256, 10 Center Drive, MSC 1074, Bethesda, Maryland 20892, and Department of Chemistry, The Pennsylvania State University, University Park, Pennsylvania 16802

Received September 26, 2001

Abstract: MS-325 is a novel blood pool contrast agent for magnetic resonance imaging currently undergoing clinical trials to assess blockage in arteries. MS-325 functions by binding to human serum albumin (HSA) in plasma. Binding to HSA serves to prolong plasma half-life, retain the agent in the blood pool, and increase the relaxation rate of water protons in plasma. Ultrafiltration studies with a 5 kDa molecular weight cutoff filter show that MS-325 binds to HSA with stepwise stoichiometric affinity constants (mM^{-1}) of K_{a1} = t t.0 ± 2.7, K_{a2} = 0.84 ± 0. t6, K_{a3} = 0.26 ± 0. t4, and K_{a4} = 0.43 ± 0.24. Under the conditions 0. t mM MS-325, 4.5% HSA, pH 7.4 (phosphate-buffered saline), and 37 °C, 88 ± 2% of MS-325 is bound to albumin. Fluorescent probe displacement studies show that MS-325 can displace dansyl sarcosine and dansyl-L-asparagine from HSA with inhibition constants (K_i) of 85 ± 3 μM and t500 ± 850 μM, respectively; however, MS-325 is unable to displace warfarin. These results suggest that MS-325 binds primarily to site II on HSA. The relaxivity of MS-325 when bound to HSA is shown to be site dependent. The Eu(III) analogue of MS-325 is shown to contain one inner-sphere water molecule in the presence and in the absence of HSA. The synthesis of an MS-325 analogue, **5**, containing no inner-sphere water molecules is described. Compound **5** is used to estimate the contribution to relaxivity from the outer-sphere water molecules surrounding MS-325. The high relaxivity of MS-325 bound to HSA is primarily because of a 60− t00-fold increase in the rotational correlation time of the molecule upon binding (τ_R = 10. t ± 2.6 ns bound vs t15 ps free). Analysis of the nuclear magnetic relaxation dispersion (T_1 and T_2) profiles also suggests a decrease in the electronic relaxation rate (t/T_{1e} at 20 MHz = 2.0 × t0^8 s^{-1} bound vs 1.1 × 10^9 s^{-1} free) and an increase in the inner-sphere water residency time (τ_m = t70 ± 40 ns bound vs 69 ± 20 ns free).

Introduction

Magnetic resonance imaging (MRI) contrast agents are unique diagnostic drugs which alter water proton relaxation times of tissue and increase contrast between normal and abnormal structures on MRI scans. While early contrast agents were simple chelates of gadolinium, more recent attempts have involved targeting the agents to particular binding sites in vivo and exploiting the unique biophysical properties inherent in the electron−nuclear interaction.[1] The most important of these features is the dependence of water relaxation on the rotational correlation time of a metal complex. Theory and early results with metal ions bound to proteins suggest that an increase in relaxivity could be obtained by protein−chelate binding.[1,2] The coupling of this biophysical trick with retention in a particular tissue, by virtue of the binding, provided a unique way to increase contrast. MS-325 is the first representative member of this class of agents targeted to the vasculature.[3,4]

Gadolinium(III) complexes function as contrast agents by shortening the T_1 of water protons wherever the complex localizes. In a T_1-weighted MR image, water molecules with the shortest T_1 will give the largest signal. Consequently, areas of the body containing contrast agent will appear as bright regions in an MR image.

All Gd(III) complexes used as contrast agents contain a common structural feature: at least one coordinated water molecule. The Gd(III) complex acts as a catalyst to relax bulk water by providing efficient relaxation of the coordinated water molecule. As this water molecule is in fast exchange with the

* To whom correspondence should be addressed. E-mail: pcaravan@epixmed.com. Fax: +1 617 250 6127.
† EPIX Medical, Inc.
‡ National Institutes of Health.
§ The Pennsylvania State University.

(1) Caravan, P.; Ellison, J. J.; McMurry, T. J.; Lauffer, R. B. *Chem. Rev.* **1999**, *99*, 2293−2352.
(2) Lauffer, R. B. *Chem. Rev.* **1987**, *87*, 901−927.
(3) Parmelee, D. J.; Walovitch, R. C.; Ouellet, H. S.; Lauffer, R. B. *Invest. Radiol.* **1997**, *32*, 741−747.
(4) Lauffer, R. B.; Parmelee, D. J.; Dunham, S. U.; Ouellet, H. S.; Dolan, R. P.; Witte, S.; McMurry, T. J.; Walovitch, R. C. *Radiology* **1998**, *207*, 529−538.

10.1021/ja017168k CCC: $22.00

Chart 1

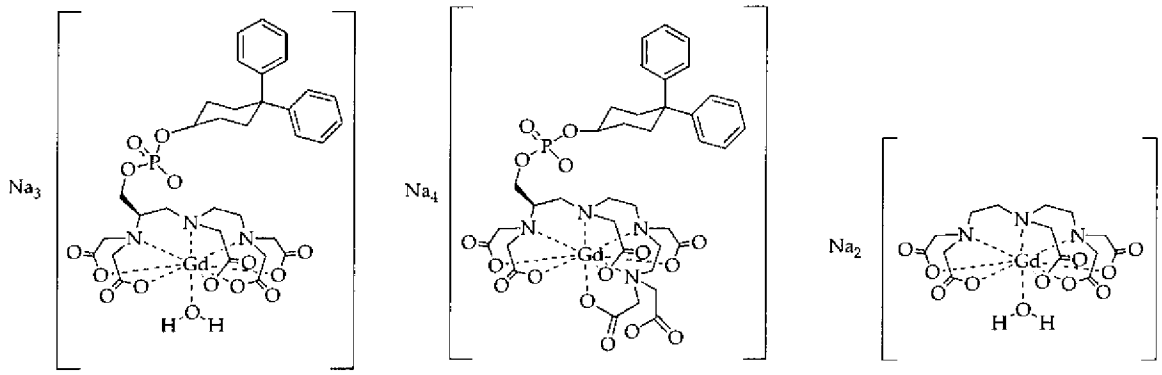

MS-325 $q = 1$ | 5 $q = 0$ | $Na_2[Gd(DTPA)(H_2O)]$ $q = 1$

bulk, the net effect is an increase in the relaxation rate of bulk water molecules, which is dependent upon the gadolinium(III) concentration, the rate of water exchange, and the rate of relaxation of the protons on the coordinated water molecule. This is often referred to as inner-sphere relaxation because it arises from a water molecule in the first coordination sphere. There is also a relaxation enhancement provided by the paramagnetic molecule to water molecules which are diffusing close to the Gd(III) ion, and to those which occupy the "second coordination sphere"; these relaxation mechanisms are different but are often grouped together as outer-sphere relaxation. For the commercially available extracellular contrast agents, the observed relaxation enhancement arises from similar outer- and inner-sphere contributions. The degree of relaxation enhancement provided by the paramagnetic ion, normalized to 1 mM, is commonly referred to as relaxivity, r_1 and r_2, where r_1 refers to longitudinal and r_2 to transverse relaxivity, respectively (eq 1).

$$(1/T_i)_{obs} = (1/T_i)_{diamagnetic} + r_i[Gd] \qquad i = 1, 2 \quad (1)$$

To effect relaxation of a coordinated water proton, a local fluctuating magnetic field is required. The gadolinium(III) ion with its seven unpaired electrons is well suited to this task. The rate at which this magnetic field fluctuates depends primarily on the rate at which the complex rotates and the rate of relaxation of the unpaired f electrons. The faster of the two rates will dominate the relaxation enhancement process. Gd(III) has a symmetric electronic ground state, ^8S, which results in a relatively slow electronic relaxation rate, especially compared to the other lanthanide(III) ions. For clinically approved contrast agents, it is primarily the rate of rotation which determines the degree of relaxation enhancement at clinical imaging field strengths.

Proton relaxation will be optimum when the fluctuating magnetic field is in resonance with the proton Larmor frequency. For clinical imaging fields which range from 0.5 to 1.5 T, this corresponds to Larmor frequencies of 20−65 MHz. Gd(III) chelates used clinically have rotational frequencies in the 1−2 GHz range. The current generation of contrast agents has far from optimal relaxation enhancing properties because of the fast rate of molecular rotation.

It was recognized early on that slowing down molecular tumbling would increase relaxivity.[2,5,6] Recent approaches for high-relaxivity agents have involved the incorporation of Gd(III) chelates into high-molecular-weight structures—either natural[7−13] or synthetic[14−20] polymers or dendrimers.[21−25] In these instances, the relaxivity increase is realized by increasing the number of Gd(III) ions per molecule and by slowing down rotation as a result of increased molecular weight. Increases in relaxation per gadolinium are generally not as great as would be expected on the basis of molecular weight because of fast segmental motions within the polymers.[1]

An alternate to the macromolecular approach is the so-called receptor-induced magnetization enhancement (RIME) strategy.[26,27] The RIME method involves targeting a small Gd(III) complex to a particular protein. Binding to a macromolecule causes an increased concentration of the Gd(III) complex in the area of the receptor molecule, giving selective enhancement of

(5) Lauffer, R. B.; Brady, T. J. *Magn. Reson. Imaging* **1985**, *3*, 11−16.
(6) Lauffer, R. B.; Brady, T. J.; Brown, R. D., III; Baglin, C.; Koenig, S. H. *Magn. Reson. Med.* **1986**, *3*, 541−548.
(7) Armitage, F. E.; Richardson, D. E.; Li, K. C. P. *Bioconjugate Chem.* **1990**, *1*, 365−374.
(8) Casali, C.; Janier, M.; Canet, E.; Obadia, J. F.; Benderbous, S.; Corot, C.; Revel, D. *Acad. Radiol.* **1998**, *5*, S214−S218.
(9) Meyer, D.; Schaefer, M.; Bonillol, A.; Beaute, S.; Chambon, C. *Invest. Radiol.* **1991**, *26*, S50−S52.
(10) Meyer, D.; Schaefer, M.; Chambon, C.; Beaute, S. *Invest. Radiol.* **1994**, *29*, S90−S92.
(11) Rebizak, R.; Schaefer, M.; Dellacherie, E. *Bioconjugate Chem.* **1997**, *8*, 605−610.
(12) Rebizak, R.; Schaefer, M.; Dellacherie, E. *Bioconjugate Chem.* **1998**, *9*, 94−99.
(13) Siauve, N.; Clement, O.; Cuenod, C.-A.; Benderbous, S.; Frija, G. *Magn. Reson. Imaging* **1996**, *14*, 381−390.
(14) Schuhmann-Giampieri, G.; Schmitt-Willich, H.; Frenzel, T.; Press, W. R.; Weinmann, H.-J. *Invest. Radiol.* **1991**, *26*, 969−974.
(15) Spanoghe, M.; Lanens, D.; Dommisse, R.; Van der Linden, A.; Alder Weireldt, F. *Magn. Reson. Imaging* **1992**, *10*, 913−917.
(16) Kellar, K. E.; Henrichs, P. M.; Hollister, R.; Koenig, S. H.; Eck, J.; Wei, D. *Magn. Reson. Med.* **1997**, *38*, 712−716.
(17) Toth, E.; Van Uffelen, L.; Helm, L.; Merbach, A. E.; Ladd, D.; Briley-Saebo, K.; Kellar, K. E. *Magn. Reson. Chem.* **1998**, *36*, S125−S134.
(18) Toth, E.; Helm, L.; Kellar, K. E.; Merbach, A. E. *Chem. Eur. J.* **1999**, *5*, in press.
(19) Aime, S.; Botta, M.; Crich, S. G.; Giovenzana, G.; Palmisano, G.; Sisti, M. *Bioconjugate Chem.* **1999**, *10*, 192−199.
(20) Bogdanov, A. A. J.; Weissleder, R.; Brady, T. J. *Adv. Drug Delivery Rev.* **1995**, *16*, 335−348.
(21) Margerum, L. D.; Campion, B. K.; Koo, M.; Shargill, N.; Lai, J.-J.; Marumoto, A.; Sontum, P. C. *J. Alloys Compd.* **1997**, *249*, 185−190.
(22) Radüchel, B.; Schmitt-Willich, H.; Platzek, J.; Ebert, W.; Frenzel, T.; Misselwitz, B.; Weinmann, H.-J. *Polym. Mater. Sci. Eng.* **1998**, *79*, 516−517.
(23) Toth, E.; Pubanz, D.; Vauthey, S.; Helm, L.; Merbach, A. E. *Chem. Eur. J.* **1996**, *2*, 1607−1615.
(24) Wiener, E. C.; Brechbiel, M. W.; Gansow, O. A.; Foley, G.; Lauterbur, P. C. *Polym. Mater. Sci. Eng.* **1997**, *77*, 193−194.
(25) Wu, C.; Brechbiel, M. W.; Kozak, R. W.; Gansow, O. A. *Bioorg. Med. Chem. Lett.* **1994**, *4*, 449−454.

the target relative to background. Unlike other imaging modalities such as X-ray and nuclear, binding also increases the signal observed (relaxation enhancement) because the Gd(III) complex now tumbles at a rotational rate that is similar to that of the target molecule. Since the relaxivity increase only occurs upon binding, there is the additional advantage of an improved target-to-background ratio.

MS-325 (Chart 1) is the first RIME contrast agent[3,4] designed to image the blood pool by exploiting noncovalent binding to the plasma protein human serum albumin (HSA). This interaction limits the amount of free drug, which can extravasate from the blood pool into nonvascular space and provides selective vascular relaxation rate enhancement. HSA, which constitutes about 4.5% of plasma (~0.67 mM), is a large (67 kDa) globular protein that is known to bind a variety of molecules (drugs, metabolites, fatty acids) at different sites on the protein.[28] Relaxation enhancement of water protons with MS-325 is much greater in plasma or in HSA solution than in pure water. Strong binding to albumin also reduces the fraction of free chelate available for glomerular filtration in the kidneys, thus slowing the renal excretion rate and contributing to an extended blood half-life. The result of this is a longer time period for imaging, which allows the radiologist to perform multiple imaging experiments and to image under steady-state conditions. MS-325 is currently undergoing Phase III clinical trials for imaging arteries and veins.

From the biophysics perspective, increasing the rotational correlation time unmasked the contributions from other parameters such as electronic relaxation and the water residency time. Although relaxivities have been reported, there have been few systematic studies to measure each of these parameters under physiologically relevant conditions.

The purpose of this paper is to identify and quantify the factors which contribute to the high relaxivity of MS-325 when it is bound to HSA. Do parameters such as water residency time and electronic relaxation also change upon binding, and if so, how do they influence relaxivity? First, the binding of MS-325 to HSA has been investigated by direct (ultrafiltration) and indirect (relaxivity) methods over a wide range of protein-to-drug ratios. Establishment of binding constants of MS-325 to HSA allows the choice of conditions whereby one MS-325 molecule is bound predominantly to a single site on HSA. Under these conditions, information on the parameters influencing relaxivity can be gleaned. To this end, variable-temperature and variable-magnetic-field ^1H and ^{17}O T_1 and T_2 relaxation measurements have been performed on MS-325 in the presence and in the absence of HSA. A related compound, **5** (Chart 1), has been prepared which contains no coordinated water molecules; this serves as an important outer-sphere control. Fluorescence lifetime measurements on the Eu(III) analogues of MS-325 in the presence and in the absence of HSA establish the inner-sphere hydration number, q, of the complexes.

Results and Discussion

Relaxation Enhancement. Proton relaxation rates were measured for MS-325 in the presence and in the absence of HSA at 20 and 64.5 MHz (0.47 and 1.50 T, respectively) at 37 °C. It was previously shown that the observed relaxation rate increases as MS-325 is added to a 4.5% solution of HSA or to a solution of phosphate-buffered saline.[4] The relaxation rate increase is much larger in the presence of HSA, and the relaxation rate does not increase linearly with concentration, indicative of protein binding.[29] To demonstrate the extent of relaxation enhancement, an ϵ^* titration is shown in Figure 1. Here, the ratio of paramagnetic relaxation rates in the presence and in the absence of HSA is plotted versus increasing HSA/MS-325 ratio, eq 2, for a constant molal concentration of MS-325. There is a 9-fold increase in relaxivity at 20 MHz upon binding to HSA and a 5-fold increase at 64 MHz.

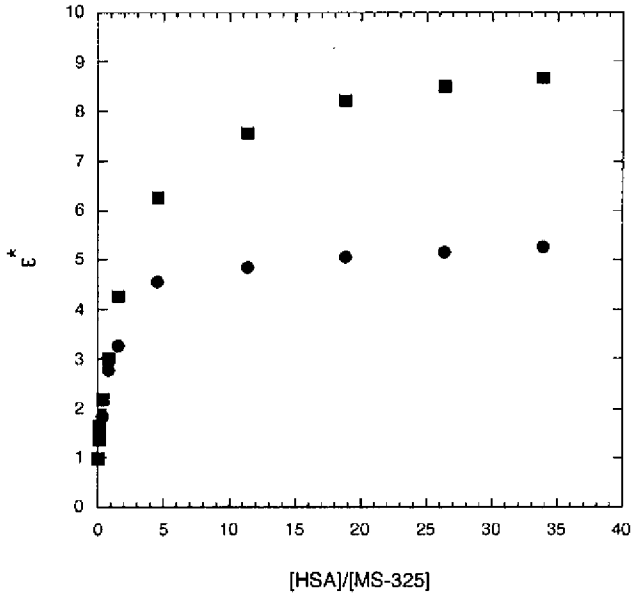

Figure 1. ϵ^* versus [HSA]/[MS-325] at 37 °C in phosphate-buffered saline (pH 7.4) for a 0.1 mmolal solution of MS-325 and 0−22.5% w/v HSA at 20 MHz (■) and 64.5 MHz (●).

$$\epsilon^* = \frac{(1/T_1)^{HSA}_{obs} - (1/T_1)^{HSA}_{dia}}{(1/T_1)^{PBS}_{obs} - (1//T_1)^{PBS}_{dia}} = \frac{(1//T_1)^{HSA}_{para}}{(1/T_1)^{PBS}_{para}} \qquad (2)$$

Albumin Binding. Before the nature of the protein-bound relaxation enhancement can be understood, the noncovalent interaction between MS-325 and HSA must be explored. Protein−complex binding was determined by ultrafiltration across a membrane with a MW 5000 cutoff. The amounts of unbound MS-325 and total MS-325 were measured directly by ICP-MS. The extent of binding of MS-325 to HSA is shown in Figure 2. The total chelate concentration ranged from 0.05 to 5.3 mM while the protein concentration was fixed at 4.5%. Under these conditions, the percent bound to HSA ranged from 88 to 37%, respectively. The data are presented in Figure 2 as a plot of the ratio of bound MS-325 per HSA molecule ($\bar{n}$) versus the concentration of unbound MS-325. It is clear from Figure 2 that $\bar{n}$ increases steeply as the molar concentration (on a logarithmic scale) increases. It is apparent that at higher free MS-325 concentrations, $\bar{n}$ would increase well above 3 equivalents bound MS-325 per HSA. A complete binding curve would show an inflection and then reverse its slope so that ultimately

(26) Jenkins, B. G.; Armstrong, E.; Lauffer, R. B. *Magn. Reson. Med.* **1991**, *17*, 164−178.
(27) Lauffer, R. B. *Magn. Reson. Med.* **1991**, *22*, 339.
(28) Peters, T. J. *All About Albumin: Biochemistry, Genetics, and Medical Applications*; Academic Press: San Diego, 1996.
(29) Dwek, R. A. *Nuclear Magnetic Resonance (N.M.R.) in Biochemistry*; Oxford University Press: Oxford, 1973.

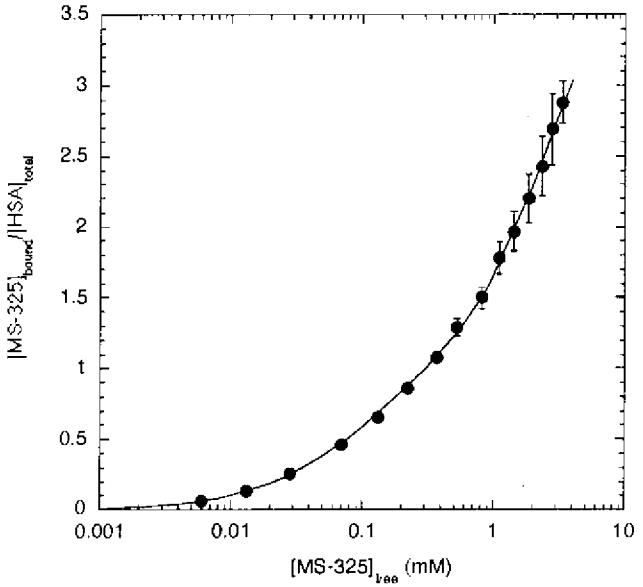

Figure 2. Binding isotherm for MS-325 (37 °C, phosphate-buffered saline, pH 7.4) to 4.5% (w/v) HSA.

a saturation plateau would appear. The value at which $\bar{n}$ reaches a plateau would give the total number of occupied sites on HSA when it is saturated with MS-325. Under the conditions employed herein, this plateau cannot be determined.

Nevertheless, one can evaluate binding constants for the earliest steps, particularly if a classical stoichiometric model of the equilibria is used. For the following stepwise equilibria,

$$\text{MS-325} + \text{HSA} \rightleftharpoons (\text{MS-325})\text{HSA}; \qquad K_1 = \frac{[(\text{MS-325})\text{HSA}]}{[\text{MS-325}][\text{HSA}]} \quad (3)$$

$$(\text{MS-325}) + (\text{MS-325})\text{HSA} \rightleftharpoons (\text{MS-325})_2\text{HSA}; \qquad K_2 = \frac{[(\text{MS-325})_2\text{HSA}]}{[\text{MS-325}][(\text{MS-325})\text{HSA}]} \quad (4)$$

$$\text{MS-325} + (\text{MS-325})_2\text{HSA} \rightleftharpoons (\text{MS-325})_3\text{HSA}; \qquad K_3 = \frac{[(\text{MS-325})_3\text{HSA}]}{[\text{MS-325}][(\text{MS-325})_2\text{HSA}]} \quad (5)$$

$$\text{MS-325} + (\text{MS-325})_3\text{HSA} \rightleftharpoons (\text{MS-325})_4\text{HSA}; \qquad K_4 = \frac{[(\text{MS-325})_4\text{HSA}]}{[\text{MS-325}][(\text{MS-325})_3\text{HSA}]} \quad (6)$$

the function $\bar{n}$ can be expressed in terms of these four association constants, eq 7, where F represents the concentration of free (unbound) MS-325. The experimental binding data were fit to

$$\bar{n} = \frac{K_1F + 2K_1K_2F^2 + 3K_1K_2K_3F^3 + 4K_1K_2K_3K_4F^4}{1 + K_1F + K_1K_2F^2 + K_1K_2K_3F^3 + K_1K_2K_3K_4F^4} \quad (7)$$

eq 7, and the stoichiometric binding constants K_2, K_3, and K_4 were evaluated (Table 1). In the fitting, K_1 was fixed to 11.0 mM^{-1}. This value was chosen based upon 36 data points (Table S1) collected in the range $0.003 < F < 0.015$ mM, since in the limit $F \rightarrow 0$, $\bar{n}/F \rightarrow K_{a1}$.[10] Table 1 also gives the corresponding free energy changes of binding, ΔG_i. It should be explicitly stated that the stoichiometric constants in Table 1 are not site binding constants, k_i. The latter cannot be addressed without additional molecular information.

Table 1. Stepwise Association Constants for the Binding of MS-325 to HSA in PBS at 37 °C[a]

binding event (i)	K_{ai} (mM^{-1})	ΔG_i° ($kJ \cdot mol^{-1}$)
1	11.0 (2.7)	24.0 (0.6)
2	0.84 (0.16)	17.5 (0.3)
3	0.26 (0.14)	14.3 (1.2)
4	0.43 (0.24)	15.6 (2.1)

[a] Numbers in parentheses represent 3σ.

Sudlow and co-workers identified two sites on HSA which bound a variety of drugs, and these were denoted site I and site II.[31,32] It has been shown that site I is a large site existing on subdomain IIA capable of binding a diverse range molecules including warfarin and salicylate. Within site I, it has been proposed that there are at least three partially overlapping regions. Yamasaki et al.[33] suggest using warfarin, dansyl-L-asparagine (DNSA), and *n*-butyl *p*-aminobenzoate as fluorescent probes of these site I regions. Site II, located on subdomain IIIA, binds diazepam, ibuprofen, and naproxen among other drugs.[28,34] Dansylsarcosine has often been used as a fluorescent probe of site II.[32]

The effect of incremental additions of MS-325 to solutions containing equal amounts of a fluorescent probe (either warfarin, DNSA, or dansylsarcosine) and HSA was studied by monitoring the change in fluorescence with added MS-325. These probes only fluoresce when they are bound to HSA, and a decrease in fluorescence is taken as displacement by MS-325. The data for these probe displacement studies are summarized in Figure 3. The graph shows probe displacement for three separate experiments; i.e., only one fluorophore is present during each titration. The decrease in fluorescence intensity, expressed as a percentage of initial fluorescence, is plotted as a function of the amount of MS-325 added. It is clear that MS-325 is most effective at displacing dansylsarcosine, the site II probe. MS-325 is a weak displacer of DNSA. Warfarin (5 μM) shows no sign of displacement from HSA (5 μM) by MS-325 at MS-325 concentrations out to 400 μM. This suggests that MS-325 binds primarily to site II and has a lower affinity for site I.

The probe displacement data can be fit to obtain an inhibition equilibrium constant, K_i, which reflects the affinity of MS-325 for a given probe's binding site (Table 2). The model used ignores MS-325 binding to sites other than that occupied by the probe: the effect that this may have on the affinity of HSA for the probe when a molecule of MS-325 is bound elsewhere, or the effect it may have on the site affinity for MS-325 when a molecule of MS-325 is already bound elsewhere, is not addressed. Despite these caveats, it is interesting to note that the affinity for the dansylsarcosine site (site II) is similar to the first stoichiometric equilibrium constant. This suggests that at

(30) Klotz, I. M. *Ligand Receptor Energetics—A Guide for the Perplexed*; John Wiley & Sons: New York, 1987.
(31) Sudlow, G.; Birkett, D. J.; Wade, D. N. *Mol. Pharmacol.* **1975**, *11*, 824–832.
(32) Sudlow, G.; Birkett, D. J.; Wade, D. N. *Mol. Pharmacol.* **1976**, *12*, 1052–1061.
(33) Yamasaki, K.; Maruyama, T.; Kragh-Hansen, U.; Otagiri, M. *Biochim. Biophys. Acta* **1996**, *1295*, 147–157.
(34) He, X. M.; Carter, D. C. *Nature* **1992**, *358*, 209–215.

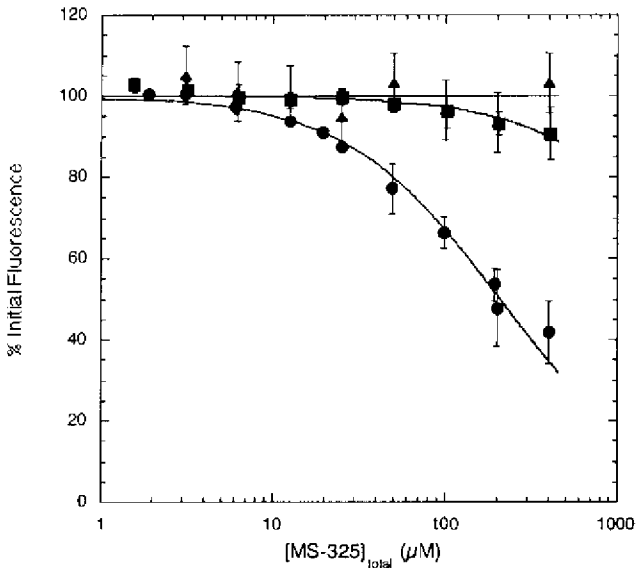

Figure 3. Summary plot of displacement of fluorescent probes dansylsarcosine (●, 5 μM), dansyl-L-asparagine (■, 15 μM), and warfarin (▲, 5 μM) from equimolar HSA by MS-325 at 37 °C, phosphate-buffered saline, pH 7.4.

Table 2. Inhibition Constants for MS-325 and **5** at 37 °C in PBS for the Displacement of Various Fluorescent Probes

	K_i		
complex	dansyl–sarcosine	dansyl-asparagine	warfarin
MS-325	85 (3)	1500 (850)	no displacement
5	62 (10)	1500 (1060)	1260 (530)

[a] Numbers in parentheses represent 3σ.

low concentrations of drug, MS-325 will be primarily bound to this high-affinity site (site II).

There have been two recent reports on the interaction of MS-325 with HSA.[35,36] In both reports an association constant was estimated from relaxation rate enhancement data assuming a model where there is only one binding site. The K_{a1} measured directly in this study using classical binding techniques is intermediate between the values determined indirectly in the previous two reports.

Site-Dependent Relaxivity. The combination of binding plus proton relaxation rate enhancement data provides a unique opportunity to evaluate the dependence of site occupancy on relaxivity. One can define an average bound relaxivity, $\bar{r}_{1b}$, which is analogous to $\bar{n}$, eq 8. For the ultrafiltration binding

$$\bar{r}_{1b} = \frac{{}^1/_{T_{1obs}} - {}^1/_{T_{1dia}} - [\mathrm{MS-325}]r_{1f}}{[\mathrm{MS-325}]_b} \qquad (8)$$

experiment summarized in Figure 2, ^{1}H relaxation rates were measured at 20 MHz. Since the concentrations of MS-325 free and bound to HSA are determined by the ultrafiltration experiment, and the relaxivity of MS-325 free, r_{1f}, is known, then the function $\bar{r}_{1b}$ can be calculated. Figure 4 shows the mean bound relaxivity as a function of total MS-325 concentration in the presence of 4.5% HSA. It is apparent from Figure 4 that

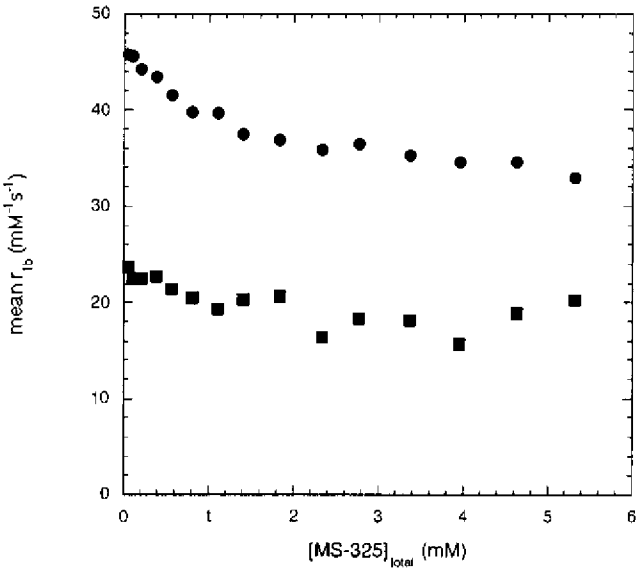

Figure 4. Mean bound relaxivity at 20 MHz (●) and 64.5 MHz (■) versus total MS-325 concentration at 37 °C, in 4.5% (w/v) HSA, phosphate-buffered saline, pH 7.4 solution.

Table 3. $\bar{r}_{1b}$ for MS-325 as $[\mathrm{MS-325}]_{free} \rightarrow 0$

frequency	$\bar{r}_{1b}$ (mM^{-1} s^{-1})
20	50.8
64.5	25.0

bound relaxivity is site dependent and variable. As the concentration of MS-325 is decreased, the mean bound relaxivity increases. This indicates that the high-affinity binding site is also a high-relaxivity site for MS-325. Combining these data with the results of the ϵ^* titration, one can estimate relaxivities at the high-affinity site for the magnetic fields used in this study. These are given in Table 3; the value at 20 MHz is similar to that reported by Muller et al.[36]

Molecular Factors Affecting Relaxivity. To better understand the mode of action of MS-325, the molecular factors which determine relaxivity were probed. As outlined in the Introduction, relaxivity depends on (1) the number of water molecules coordinated in the inner-sphere, (2) the rate of water exchange, (3) the electronic relaxation rate of the Gd(III) ion, (4) the rotational diffusion time of the Gd–H vector, and (5) the so-called outer-sphere relaxivity wherein the Gd ion relaxes water molecules not directly coordinated to it.

Hydration Number. Fluorescence lifetime experiments were performed on the Eu(III) analogue of MS-325 in H_2O and D_2O solutions in the presence and in the absence of HSA. It is well established that the ratio of fluorescence decay constants in both solvents is proportional to q, the hydration number of the complex.[37,38] Hydration numbers are given in Table 4 and demonstrate that MS-325 has one coordinated water molecule either free in PBS buffer or when bound to HSA.

Outer-Sphere Relaxivity. To estimate the extent of outer-sphere relaxivity, the $q = 0$ analogue **5** (Scheme 1) was synthesized. The synthesis of **5** commenced by coupling

(35) Aime, S.; Chiaussa, M.; Digilio, G.; Gianolio, E.; Terreno, E. *JBIC, J. Biol. Inorg. Chem.* **1999**, *4*, 766–774.
(36) Muller, R. N.; Radüchel, B.; Laurent, S.; Platzek, J.; Pierart, C.; Mareski, P.; Vander Elst, L. *Eur. J. Inorg. Chem.* **1999**, 1949–1955.
(37) (a) Horrocks, W. DeW., Jr.; Sudnick, D. R. *J. Am. Chem. Soc.* **1979**, *101*, 334–340. (b) Supkowski, R. M.; Horrocks, W. DeW., Jr. *Inorg. Chem.* **1999**, *38*, 5616–5619.
(38) Beeby, A.; Clarkson, I. M.; Dickins, R. S.; Faulkner, S.; Parker, D.; Royle, L.; de Sousa, A. S.; Williams, J. A. G.; Woods, M. *J. Chem. Soc., Perkin Trans. 2* **1999**, 493–504.

Scheme 1

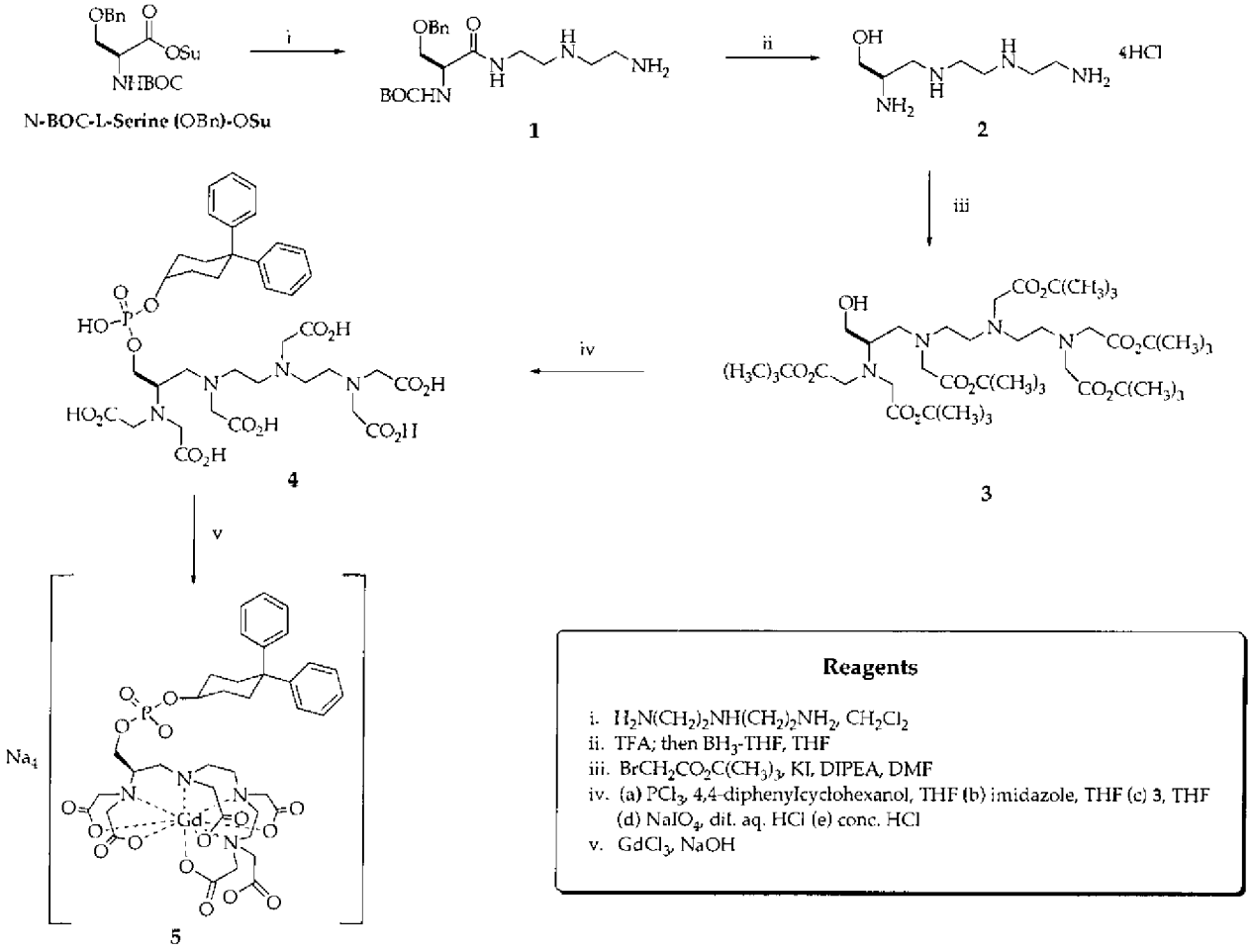

Table 4. Hydration Numbers of the Eu(III) Analogues of MS-325 and **5** in HEPES buffer (pH 7.0) or in 4.5% HSA/HEPES Buffer Solution at 37 °C

	lifetime (μs)		
system	H_2O	D_2O	q
MS-325/HEPES	597	2199	1.02
MS-325/HSA	654.4	2535	0.93
5/HEPES	1222	1928	0.0
5/HSA	1307	1933	−0.06

[a] $q = \tau_{H_2O}^{-1} - \tau_{D_2O}^{-1} - 0.30$; τ = lifetime in ms.[37b]

N-BOC-L-serine(Obn)-OSu to triethylenetriamine. The resultant amide was treated with TFA, then borane−tetrahydrofuran complex to furnish amine **2**, which was alkylated with *tert*-butyl bromoacetate, providing the alcohol hexaester **3**. A phosphorylation sequence utilizing phosphorous trichloride and **3**, followed by chelation with gadolinium chloride, yielded **5**.

Compound **5** is based on the well-studied triethylenetetraamine hexaacetate (TTHA) ligand core, which is known to coordinatively saturate lanthanide(III) ions.[39−44] Complex **5** has a slightly higher affinity for HSA than MS-325 (95% bound at 0.1 mM **5**, 4.5% HSA vs 88% for MS-325 under the same conditions). It also binds to site II, as evinced from fluorescent probe displacement studies (K_i values given in Table 2). Luminescence lifetime measurements established that the Eu(III) analogue of **5** has no inner-sphere water molecule in the presence or in the absence of HSA (Table 4).

Inner-Sphere Relaxivity. Longitudinal (r_1) and transverse (r_2) molal relaxivities were measured for MS-325 and **5** over the ^{1}H Larmor frequency range 4−64 MHz using 0.1 mmolal Gd in the presence and in the absence of 22.5% HSA. A high (~34:1) protein-to-drug ratio was used in order to maximize the amount of drug bound to HSA and also to maximize the amount of drug bound in the highest affinity site. Plots of molal relaxivity for MS-325 and **5** with and without HSA are shown in Figures 5 and 6, respectively. In the presence of HSA, the relaxivity of MS-325 increases dramatically: the r_1 curve increasing and then decreasing with field, typical of a slow rotating molecule, and the r_2 curve rising to a maximum and then reaching a plateau. The relaxivity of **5** also increases upon binding to HSA; although the effect is not as dramatic as that of MS-325, there is still a 2−4-fold increase depending on field.

To ascertain the amount of relaxivity conferred to the solvent by the inner-sphere water molecule on MS-325, an inner-sphere bound relaxivity was calculated. First, $\bar{r}_{1,2b}$ was calculated for

(39) Alpoim, M. C.; Urbano, A. M.; Geraldes, C. F. G. C.; Peters, J. A. *J. Chem. Soc., Dalton Trans.* **1992**, 463−467.
(40) Chang, C. A.; Brittain, H. G.; Telser, J.; Tweedle, M. F. *Inorg. Chem.* **1990**, *29*, 4468−4473.
(41) Ruloff, R.; Gelbrich, T.; Sieler, J.; Hoyer, E.; Beyer, L. *Z. Naturforsch., B: Chem. Sci.* **1997**, *52*, 805−809.
(42) Ruloff, R.; Prokop, P.; Sieler, J.; Hoyer, E.; Beyer, L. *Z. Naturforsch., B: Chem. Sci.* **1996**, *51*, 963−968.
(43) Wang, R.-Y.; Li, J.-R.; Jin, T.-Z.; Xu, G.-X.; Zhou, Z.-Y.; Zhou, X.-G. *Polyhedron* **1997**, *16*, 1361−1364.
(44) Wang, R.-Y.; Li, J.-R.; Jin, T.-Z.; Xu, G.-X.; Zhou, Z.-Y.; Zhou, X.-G. *Polyhedron* **1997**, *16*, 2037−2040.

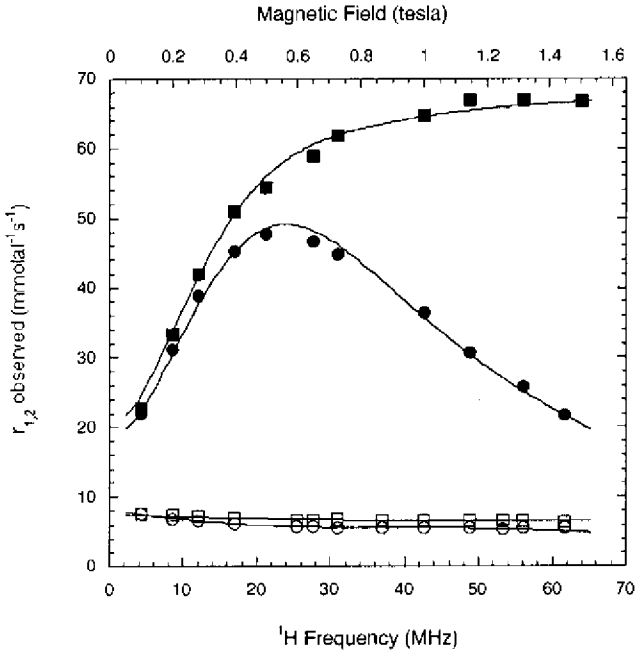

Figure 5. Observed longitudinal (r_1^{obs}, circles) and transverse (r_2^{obs}, squares) relaxivity for 0.1 mmolal MS-325 in the presence (filled symbols) and in the absence (open symbols) of 22.5% (w/v) HSA at 37 °C, phosphate-buffered saline, pH 7.4. Solid lines are fits to the data as described in the text.

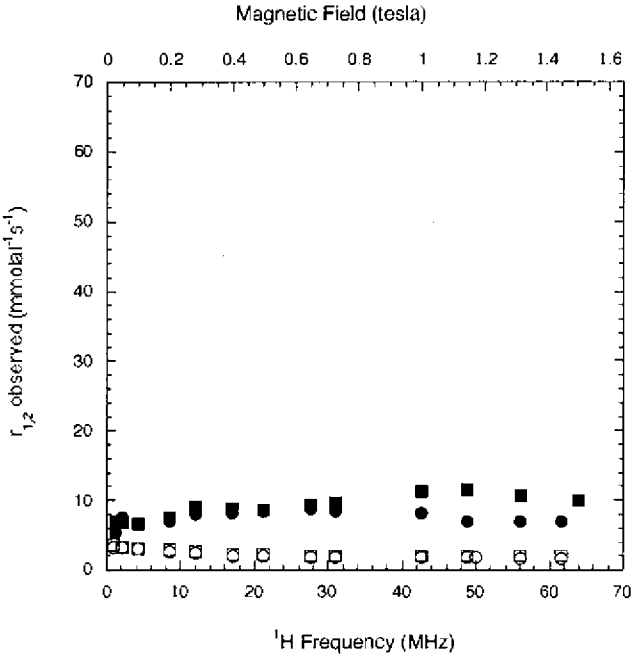

Figure 6. Observed longitudinal (r_1^{obs}, circles) and transverse (r_2^{obs}, squares) relaxivity for 0.1 mmolal **5** in the presence (filled symbols) and in the absence (open symbols) of 22.5% (w/v) HSA at 37 °C, phosphate-buffered saline, pH 7.4.

both MS-325 and **5** since both the relaxivity free and the concentration free (from ultrafiltration binding studies) were known. Since **5** is chemically very similar to MS-325 (it has the same donor atom set except that a carboxylato oxygen replaces a water oxygen, and it binds to the same site on HSA), it was assumed that the relaxivity of **5** bound to HSA reflected the outer-sphere contribution to relaxivity for MS-325. Thus, the inner-sphere bound relaxivity, $\bar{r}_{1,2b}^{IS}$, for MS-325 is given by eq 9.

$$\bar{r}_{1,2b}^{IS} = \bar{r}_{1,2b}^{MS-325} - \bar{r}_{1,2b}^{5} \quad (9)$$

Once the inner-sphere bound relaxivity has been calculated, the r_1 and r_2 curves can be fit to the Solomon–Bloembergen–Morgan equations (see Supporting Information) which describe paramagnetic relaxation.[45] Both transverse and longitudinal relaxation rate data were fit simultaneously to a dipolar relaxation mechanism allowing for chemical exchange. In total, four parameters were varied: τ_m, the water residency time; τ_R, the rotational correlation time which describes the rotational diffusion of the Gd–H vector; Δ_t^2, the square of the trace of the transient zero-field-splitting (ZFS) tensor, which is a measure of how much the electronic structure of the Gd ion is transiently distorted from spherical symmetry; and τ_v, a correlation time which describes the modulation of the transient ZFS. The latter two parameters define electronic relaxation, $T_{1,2e}$. In the fitting, the electron spin–nuclear spin distance, r_{Gd-H}, was fixed at 3.1 Å. This can also be allowed to vary. Finally, at higher fields a scalar relaxation mechanism may contribute to $1/T_2$. This mechanism involves the Gd–H hyperfine coupling constant $A^H/\hbar$. Table 5 shows results for the four-, five-, and six-parameter fits. Introduction of additional parameters did not significantly improve the fits, and the original four fitted parameters are largely unchanged.

Table 5. Four-, Five-, and Six-Parameter Fits of the NMRD Data at 37 °C in PBS, 22.5% HSA, 0.1 mmolal MS-325[a]

	four-parameter	five-parameter	six-parameter
τ_m (ns)	207 (200–213)	172 (130–213)	192 (144–240)
τ_v (ps)	21 (18–24)	20 (17–23)	23 (19–27)
Δ^2 ($\times 10^{18}$ s^{-2})	8.1 (7.6–8.6)	7.0 (5.9–8.1)	7.1 (5.7–8.4)
τ_R (ns)	13.3 (11.6–15.1)	10.1 (7.4–12.9)	9.4 (6.6–12.1)
r_{Gd-H} (Å)	3.10 (fixed)	3.19 (3.10–3.29)	3.17 (3.06–3.28)
$A/\hbar$ ($\times 10^6$ rad/s)	0 (fixed)	0 (fixed)	3.1 (1.2–5.1)

[a] Numbers in parentheses represent 95% confidence range.

Comparison with Unbound MS-325. To understand which parameters change upon binding to HSA, variable-temperature ^{1}H and ^{17}O relaxation measurements were carried out on MS-325 in the absence of HSA. Merbach and co-workers have established that ^{17}O relaxation rates for Gd complexes are determined solely by inner-sphere mechanisms;[46] this is not true of ^{1}H relaxation rates for rapidly tumbling molecules, where outer-sphere contributions can contribute up to 50% of the observed relaxation rate.[1] T_2 and chemical shift measurements of $H_2{}^{17}O$ at high field (7.05 T in this instance) yield information on the water exchange rate and T_{1e} of the Gd ion. The $1/T_2$ curve versus temperature was parabolic, with a maximum at ca. 30 °C (Figure 7). On the low-temperature side of the maximum, the transverse relaxation rate is dominated by water exchange, and the slope at the low-temperature extreme gives the activation enthalpy for exchange. At higher temperatures, $1/T_2$ is modulated by both electronic relaxation and exchange. Because only one field strength was used, the electronic relaxation rate was calculated at each temperature and assumed to have an exponential temperature dependence given by $\Delta E_{T_{1e}}$.

(45) Bertini, I.; Luchinat, C. *Coord. Chem. Rev.* **1996**, *150*, 1–295.

(46) Micskei, K.; Helm, L.; Brucher, E.; Merbach, A. E. *Inorg. Chem.* **1993**, *32*, 3844–3850.

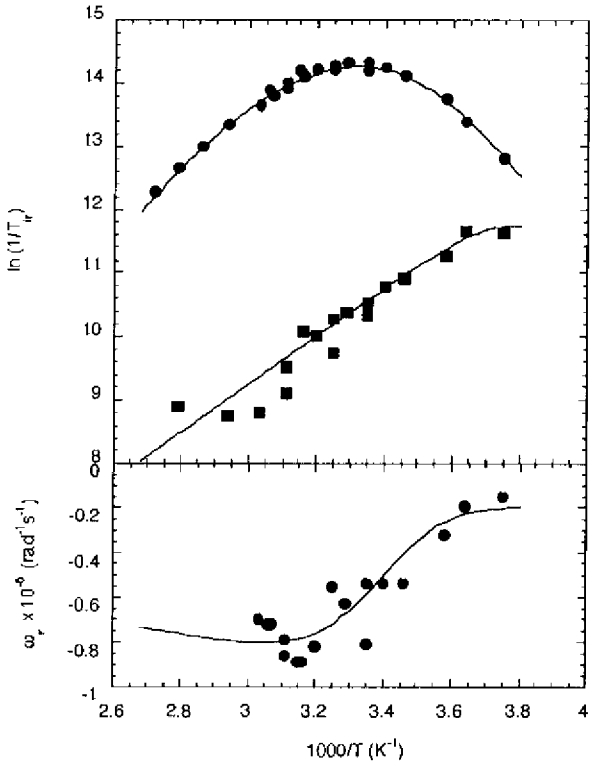

Figure 7. Reduced ^{17}O relaxation rates ($1/T_{1r}$ and $1/T_{2r}$) and chemical shifts (ω_r) of $H_2{}^{17}O$ in the presence of MS-325 in phosphate-buffered saline, pH 7.4, as function of reciprocal temperature. Solid lines represent the simultaneous fit to the data as described in the Experimental Section.

The hyperfine coupling constant, $A^o/\hbar$, between the electron spin and the ^{17}O nucleus was determined primarily through chemical shift measurements, although the T_1, T_2, and chemical shift data were fit simultaneously. The Gd T_1 measurements on $H_2{}^{17}O$ yield the rotational correlation time, provided the gadolinium–water oxygen distance is known and the nuclear quadrupolar coupling constant for $H_2{}^{17}O$ coordinated to Gd is known. The distance r_{Gd-O} was set to 2.48 Å, which is the value determined from the X-ray crystal structure of MS-325.[47] The nuclear quadrupolar coupling constant was assumed to be the same as that determined for $[Gd(DTPA)(H_2O)]^{2-}$ by Powell et al.[48]

The water residency time for MS-325 is shorter than that of $[Gd(DTPA)(H_2O)]^{2-}$ (Table 6).[48] This difference is significant: there is ca. a 5 K shift to lower temperature for the $1/T_2$ maximum for MS-325 compared to $[Gd(DTPA)(H_2O)]^{2-}$ measured under identical conditions (Table S2, Supporting Information). While the water exchange rate increases upon introduction of the phosphodiester functionality on the DTPA backbone, there appears to be no difference in the electronic relaxation rate, $1/T_{1e}$, at 7.05 T between MS-325 and $[Gd(DTPA)(H_2O)]^{2-}$. The water exchange rate determined here for MS-325 is in good agreement with that published by Muller et al.,[36] and the water exchange rate for $[Gd(DTPA)(H_2O)]^{2-}$ is in good agreement with that reported by Powell et al.[48]

The rotational correlation time at 37 °C is about 120 ps (Table 6). Analysis of the ^{17}O T_1 data gives 115 ps, while ^1H T_1 and T_2 data give 125 ps using a Gd–H distance of 3.1 Å. Proton relaxivity at fields >0.5 T is determined by the rotational correlation time and the electron spin–nuclear spin distance, and these two parameters are strongly correlated; decreasing (increasing) r_{Gd-H} by 0.1 Å decreases (increases) τ_R by 25 ps. A τ_R of 117 ps was reported for the La analogue of MS-325 determined by ^2H NMR at 37 °C.[36]

Table 6. Parameters Obtained from the Simultaneous Fit of T_1, T_2, and Chemical Shift Data for $H_2{}^{17}O$ in the Presence of MS-325 or Magnevist and Literature Values[a]

	this work	ref 36	ref 35	Magnevist[b,c]
$\tau_m{}^{37}$ (ns)	69 (20)	83	105	140,[b] 130[c]
$k_{ex}{}^{298}$ ($\times 10^6$ s^{-1})	5.8 (0.6)	5.1	4.0	3.1,[b] 3.3[c]
$\Delta H^{\ddagger}$ (kJ mol^{-1})	53.7 (5.6)	51.3	53.0	55.7,[b] 51.6[c]
$\Delta S^{\ddagger}$ (J K^{-1}mol^{-1})	+65 (10)	+51.3	+59.0	+66,[b] +53.0[b]
$1/T_{1e}{}^{37}$($\times 10^7$ s^{-1})	5.0 (2.6)	3.6	17.0	3.2[b]
$\Delta E_{T_{1e}}$ (kJ mol^{-1})	−7.7 (14.5)	6.4	10.0 (fixed)	−12.5[b]
$\tau_R{}^{37}$ (ps)	115 (10)	117	NR	44[c]
ΔE_R (kJ mol^{-1})	31.5 (3.0)	NR	NR	17.3[c]
$A/\hbar$ ($\times 10^6$ rad/s)	−4.46 (1.2)	−4.1	−3.8 (fixed)	−3.8[c] (fixed)[b]
C_{os}	0.23 (0.14)	NR	NR	0.18[c]

[a] Numbers in parentheses represent 3σ. [b] This work, [c] Reference 48. NR = not reported.

Why Binding to HSA Increases Relaxivity. The increase in relaxivity upon HSA binding is primarily because of a dramatic reduction in the rotational diffusion rate of the molecule. The rotational rate is decreased by almost a factor of 100. There are two other favorable interactions. The outer-sphere relaxivity increases by a factor of 2–4, which may be due to the presence of a long-lived (>1 ns) water molecule in the second coordination sphere. The electronic relaxation rate, $1/T_{1e}$, also slows down upon binding. On the other hand, the water exchange rate is slowed by a factor of 2–3, which limits the amount of relaxation enhancement observed.

The rotational correlation time reported here (~10 ± 3 ns) is longer than that reported by Muller et al.,[36] but the NMRD profiles are very similar in shape and magnitude. These authors give values of 3.3 and 4.4 ns for τ_R determined by ^1H NMRD and 6–7 ns for τ_R determined from ^2H line broadening studies. The rotational correlation time determined in this study is more in line with their ^2H result than their NMRD analysis. However, under the conditions employed in their study, a considerable amount of MS-325 (28%) is unbound, implying that the mean bound relaxivity (cf. Figure 4) is lower. It is likely that these authors were interpreting data in a region where the distribution of MS-325 bound to HSA was spread over several sites. In addition, these authors may have underestimated the outer-sphere contribution as compared to what was experimentally observed for **5**. These authors also assume that the water exchange rate does not change upon binding; this will have the effect of shortening τ_R in the fitting procedure. On the other hand, the higher protein concentration in this study may alter the microviscosity such that rotation within the whole system is slowed. Stanisz and Henkelman[49] have shown that increasing amounts of macromolecule can increase the relaxation enhancement of water by $[Gd(DTPA)(H_2O)]^{2-}$, although there is no specific interaction between the macromolecule and the metal complex. The difference in microviscosity may slow the rotational rate by as much as 50% upon increasing the protein content from 4 to 22.5%.

(47) Tyeklar, Z.; Midelfort, K.; Dunham, S.; Lauffer, R.; McMurry, T.; Hollander, F., unpublished results.
(48) Powell, D. H.; Ni Dhubhghaill, O. M.; Pubanz, D.; Helm, L.; Lebedev, Y. S.; Schlaepfer, W.; Merbach, A. E. *J. Am. Chem. Soc.* **1996**, *118*, 9333–9346.
(49) Stanisz, G. J.; Henkelman, R. M. *Magn. Reson. Med.* **2000**, *44*, 665–667.

The increased outer-sphere relaxivity upon binding is likely because of long-lived (~1 ns) water molecule(s) in close proximity (<5 Å) to the Gd(III) ion. This effect has been observed previously by others on $q = 0$ complexes.[50,51] The $q = 0$ Mn(II) analogue of MS-325 also shows an increased relaxivity upon HSA binding.[52]

The slower electronic relaxation rate upon binding is an unexpected benefit. If the electronic relaxation parameters were identical to those reported for $[Gd(DTPA)]^{2-}$,[48] then the r_1 peak maximum in Figure 5 would occur at a higher frequency (40–45 MHz), and its amplitude would be lower. Apart from molecular symmetry, there are no predictors of electronic relaxation in Gd(III) complexes. It is unclear why the electronic relaxation rate of the Gd(III) ion should change when its complex is associated with HSA (Gd(III) electronic relaxation is not modulated by rotation). One possible explanation may lie in the determination of the electronic parameters. For fast tumbling $[Gd(DTPA)]^{2-}$, relaxation at higher fields is determined primarily by the rotational rate of the molecule; the electronic parameters Δ_t^2 and τ_v are determined from modeling the low-field relaxivity data to the SBM equations. However, at low fields the SBM equations may not be valid for this non-spherically-symmetric molecule. When the rotational rate is much slower, as is the case here, the electronic relaxation rate (which decreases with the square of the magnetic field) continues to influence the relaxivity of the complex at higher fields (where the SBM equations are valid). In this study, Δ_t^2 and τ_v were determined over the frequency range 4–64 MHz, while for $[Gd(DTPA)]^{2-}$, these parameters were determined in the range 0.01–4 MHz. It may be that the electronic relaxation rate does not change upon HSA binding; rather, the difference in electronic parameters may be due to the method used to determine them.

The apparent decrease in the water exchange rate is also somewhat surprising. This change in τ_m was also noted by Aime et al.,[35] even though these authors were working under conditions where several equivalents of MS-325 were bound to albumin. The mechanism of this is unclear. It is known that $[Gd(DTPA)(H_2O)]^{2-}$ exchanges water via a dissociative mechanism,[48] and as the activation parameters for MS-325 in the absence of protein are similar to those of $[Gd(DTPA)(H_2O)]^{2-}$, it is highly likely that MS-325 also has a dissociative water exchange mechanism.

The NMRD data were fit to an isotropic model. Strictly speaking, this is invalid. However, the data fit quite well to this model; a large degree of anisotropy would noticeably alter the shape of the dispersion profile. In addition, the X-band EPR spectrum of vanadyl-labeled MS-325 in HSA is very isotropic, suggesting that the bound Gd(III) complex here tumbles in an isotropic fashion.[53] One consequence of a small degree of anisotropy would be to lower the relaxivity. From the present data, it is impossible to distinguish a small degree of rotational anisotropy from a lengthening of the water residency time. While it is likely that the water exchange rate slows down upon HSA binding, this has not been unequivocally shown.

Conclusion

MS-325 functions as a contrast agent by targeting HSA in blood. The affinity for HSA is moderate: at typical circulating concentrations of 0.1 mM, 88% of the complex is noncovalently bound to HSA. Binding to HSA causes a dramatic increase in the relaxivity of the molecule, a 9-fold increase at 20 MHz. It was shown that MS-325 binds preferentially to the site II region of HSA and that this high-affinity site is also a high-relaxivity site. The relaxivity increase is primarily a result of slow rotational diffusion of the molecule upon binding to HSA.

Experimental Section

Materials. Human serum albumin (HSA), product no. A-1653 (Fraction V Powder 96–99% albumin, containing fatty acids), and HSA absorbance standards, along with the fluorescent probes dansyl L-asparagine, dansylsarcosine (piperidinium salt), and warfarin (sodium salt), were purchased from Sigma Chemical Co. (St. Louis, Mo.). Ultrafiltration units (UFC3LCC00, regenerated cellulose membrane of 5000 Da nominal molecular weight cutoff) were obtained from Millipore Corp. (Bedford, MA). Other reagents were supplied by Aldrich Chemical Co., Inc., and were used without further purification. Solvents (HPLC grade) were purchased from various commercial suppliers and used as received. Column chromatography was conducted using silica gel from EM Merck. The gadolinium sodium salt of MS-325 was prepared by Raylo Chemicals (Alberta, Canada); this was formulated in-house at a concentration of 243 mM.

Concentrations. All gadolinium concentrations were determined by ICP-MS on a PE-SCIEX ELAN 5000 system.

Synthesis. Intermediates and compounds were characterized by NMR with a Varian Unity 300 NMR spectrometer. HPLC purity analysis (both UV and MS detection) was carried out with a HP-1100 MSD system using a gradient of 20 mM ammonium formate (pH 6.8) with 5% (9:1 ACN:20 mM ammonium formate) to 95% (9:1 ACN:20 mM ammonium formate) over 12 min (0.8 mL/min, Vydac C4, 4.6 × 250 mm).

***(S)*-{1-[2-(2-Aminoethylamino)ethylcarbamoyl]-2-hydroxyethyl}-carbamic Acid *tert*-Butyl Ester, 1.** A suitable reaction flask, equipped with an addition funnel, nitrogen inlet, and temperature probe, was charged with diethylenetriamine (17.6 g, 170.1 mmol, 10 equiv). To the flask was added a mixture consisting of N-Boc-L-serine (OBzl)-OSu (6.7 g, 17.1 mmol, 1.0 equiv) and CH_2Cl_2 (40 mL) over a period of 40 min while maintaining an internal temperature 0–5 °C. The mixture was allowed to stir while warming to room temperature and stirred for an additional 3.0 h. The reaction mixture was diluted with water (50 mL) and stirred for 20 min. The layers were separated, and the organic layer was concentrated under vacuum (40–45 °C water bath, 10–15 mmHg) to provide a colorless foam (5.9 g). The foam was purified by preparative HPLC chromatography (ACN:water:0.1% TFA, C18 Vydac column) to provide 1 (2.7 g). ^1H NMR (300 MHz, $CDCl_3$): δ 7.3 (m, 5H), 7.2 (br s, 1H), 5.5 (d, $J = 6.8$, 1H), 4.54–4.44 (q, $J = 11.8$ Hz, 2H), 4.2 (br s, 1H), 3.88–3.83 (dd, $J = 3.9$ and 5.3 Hz, 1H), 3.58–3.53 (q, $J = 6.0$ Hz, 1H), 3.35–3.29 (q, $J = 11.5$ Hz, 2H), 2.6 (m, 4H), 2.5 (m, 2H), 1.4 (s, 9H), 1.3 (m, 3H). ^{13}C NMR (75 MHz, $CDCl_3$): δ 169.4, 154.6, 136.6, 127.5, 126.9 (2), 126.7 (2), 79.2, 72.4, 69.1, 53.2, 50.9, 47.3, 40.6, 38.3. MS (*m/z*): M + 1 = 381.

***(R)*-2-Amino-3-[2-(2-aminoethylamino)ethylamino]propan-1-ol Tetrahydrochloride Salt, 2.** A suitable reaction flask was charged with amide 1 (5.9 g) and 10 mL of trifluoroacetic acid (TFA). The mixture was stirred for 2.0 h at room temperature. The mixture was concentrated under reduced pressure to give an oil. The oil was triturated with diethyl ether. The solid was collected and dried until a constant weight to give a sticky white foam (5.9 g). The foam was combined with MeOH (50

(50) Aime, S.; Batsanov, A. S.; Botta, M.; Howard, J. A. K.; Parker, D.; Senanayake, K.; Williams, G. *Inorg. Chem.* **1994**, *33*, 4696–4706.
(51) Aime, S.; Botta, M.; Crich, S. G.; Giovenzana, G. B.; Pagliarin, R.; Piccinini, M.; Sisti, M.; Terreno, E. *J. Biol. Inorg. Chem.* **1997**, *2*, 470–479.
(52) Dunham, S. U.; Caravan, P., unpublished results.
(53) Clarkson, R. B.; Caravan, P., unpublished results.
(54) Banci, L.; Bertini, I.; Luchinat, C. *Nuclear and Electron Relaxation*; VCH: Weinheim, 1991.
(55) Toth, E.; Helm, L.; Merbach, A. E.; Hedinger, R.; Hegetschweiler, K.; Janossy, A. *Inorg. Chem.* **1998**, *37*, 4104–4113.

mL) and Amberlite IRA-440C (hydroxide form) resin (which was previously washed with H_2O, H_2O/MeOH (1:1), and MeOH). The slurry was stirred for 1.5 h and filtered. The resin was washed with MeOH (2 × 50 mL), and the combined filtrates were concentrated under reduced pressure to give an oil. The oil was diluted with THF (50 mL) and concentrated under reduced pressure (this removed traces of methanol) to provide an oil (2.3 g).

The oil (2.2 g) was transferred to a reaction flask equipped with an addition funnel, temperature probe, and nitrogen inlet and diluted with THF (50 mL). To the mixture was added BH_3·THF (1.6 L of a 1 M solution in THF, 50 mL) over a period of 30 min while maintaining an internal temperature of 25−35 °C. The mixture was heated to reflux, stirred for 18 h, and then cooled to 0−5 °C. A solution of 2 M HCl (50 mL) was added over 30 min while maintaining an internal temperature of 0−5 °C, followed by addition of concentrated HCl (50 mL) over a period of 20 min while maintaining an internal temperature of 0−5 °C. The mixture was warmed to room temperature and concentrated under reduced pressure until 50 mL of solution remained. The solution was refluxed at 6 h and then concentrated under reduced pressure until 10 mL of solution remained. The solution was diluted with EtOH (10 mL) and stirred at room temperature for 1.0 h. Additional EtOH was added until the solution became cloudy, and the solution was concentrated under reduced pressure to give an oil. The oil was triturated with diethyl ether to give a solid. The solid was collected by filtration and dried until a constant weight to give a sticky white powder (hydroscopic, 1.8 g). ^{1}H NMR (300 MHz, D_2O): δ 3.77−3.64 (m, 3H), 3.57−3.14 (m, 10 H). ^{13}C NMR (75 MHz, D_2O): δ 59.1, 49.2, 47.0, 44.7, 44.0, 43.4, 35.4. MS (*m/z*): M + 1 = 177.15.

[[2-(Bis-*tert*-butoxycarbonylmethylamino)ethyl]-(2-{[2-(bis-*tert*-butyoxycarbonylmethylamino)-3-hydroxypropyl]-*tert*-butoxycarbonylmethylamino}ethyl)amino]acetic Acid *tert*-Butyl Ester, 3. A reaction flask equipped with a nitrogen inlet, addition funnel, and temperature probe was charged with **2** (1.7 g, 5.3 mmol, 1.0 equiv), KI (0.88 g, 10.6 mmol, 2.0 equiv), diisopropylethylamine (12.9 mL, 74.2 mmol, 14.0 equiv), and DMF (40 mL). The mixture was warmed to 45−50 °C, and *tert*-butyl bromoacetate (5.5 mL, 37.1 mmol, 7.0 equiv) was added while maintaining an internal temperature of 45−50 °C. The reaction mixture was stirred for 18 h and then cooled to room temperature. Ethyl acetate (80 mL) and water (80 mL) were added, and the mixture was stirred for 15 min. The layers were separated, and the organic layer was concentrated under reduced pressure to provide an oil. The oil was purified by flash column chromatography (30 g of silica gel, hexane/IPA). The fractions containing only desired product were combined to provide **3** as an oil (0.3 g). ^{1}H NMR (300 MHz, $CDCl_3$): δ 1.4 (br s, 54H), 2.5−2.4 (dd, J = 9.2 and 3.7 Hz, 1H), 2.6−2.9 (m, 10H), 3.2−3.5 (m, 13 H), 3.6 (dd, J = 4.5 and 6.8 Hz, 1H). MS (*m/z*): M + 1 = 861.

(*R*)-[[2-(Carboxymethyl-{2-dicarboxymethylamino-3-[(4,4-diphenylcyclohexyloxy)hydroxyphosphoryloxy]propyl}amino)ethyl]-(2-dicarboxymethylaminoethyl)amino]acetic Acid, 4. A reaction flask, equipped with a nitrogen inlet, temperature probe, and addition funnel, was charged with PCl_3 (0.61 mL, 7.08 mmol, 1.0 equiv) and THF (12 mL). A solution consisting of 4,4-diphenylcyclohexanol (1.78 g, 7.08 mmol, 1.0 equiv) in THF (15 mL) was added over a period of 20 min while maintaining an internal temperature of −6 to 0 °C. The mixture was stirred for 30 min. A solution consisting of imidazole (2.4 g, 35.4 mmol, 5.0 equiv) in THF (15 mL) was added over a period of 15 min while maintaining an internal temperature of −6 to 0 °C. The mixture was stirred for 30 min. A solution consisting of alcohol **3** (5.48 g, 6.4 mmol, 0.9 equiv) in THF (12 mL) was added over a period of 30 min while maintaining an internal temperature of −6 to 0 °C. The mixture was stirred for 30 min. Water (12 mL) was added all at once while maintaining an internal temperature of −6 to 6 °C. The mixture was stirred for 5 min. Heptane (36 mL), toluene (4 mL), and 5 M HCl (12 mL) were added over 5 min while maintaining an internal temperature of 6−12 °C. Sodium periodate (1.2 g, 5.7 mmol, 0.8 equiv) was added over a period of 3 min while maintaining an internal temperature of 12−15 °C. The reaction mixture was warmed to room temperature and stirred for 2.5 h. The layers were separated, and the organic layer was washed with 10% aqueous sodium thiosulfate (2 × 75 mL).

To the above organic layer was added tetraoctylammonium bromide (0.39 g, 0.708 mmol, 0.1 equiv), followed by concentrated HCl (11.51 M, 21 mL) over a period of 22 min while maintaining an internal temperature of 22−35 °C. The mixture was stirred for 16.0 h at room temperature. The layers were separated, and the organic layer was discarded.

To the above aqueous layer was added 8 M NaOH until a pH of 6.8 was achieved. The solution was concentrated under reduced pressure (50−55 °C, vacuum 85 mmHg) until a volume of 80 mL. The solution was loaded onto C-18 reversed-phase silica gel (50 g, packed wet in MeOH and then washed with 200 mL of MeOH, 200 mL of MeOH/H_2O (1:1), and finally 200 mL of H_2O) and eluted with water. The first 225 mL collected was discarded, and the next 225 mL collected was retained.

To the above retained solution was added 6 M HCl until a pH of 1.63 was achieved. The formed slurry was stirred for 1 h and filtered. The solid was washed with pH 1.67 aqueous solution and dried (48−50 °C, 4−6 mmHg) to a constant weight (18.0 h) to obtain **4** as an off-white solid (0.9 g). ^{1}H NMR (300 MHz, D_2O): δ 7.4−7.2 (m, 10H), 4.2 (br s, 1H), 3.8 (s, 2H), 3.4−2.8 (m, 13H), 2.75−2.25 (m, 11H), 2.20−2.15 (m, 3H), 1.9 (br d, 2H), 1.7 (m, 2H). ^{31}P (121 MHz, D_2O/phosphoric acid): δ −5.5. MS (*m/z*): M + 1 = 839.35.

Tetrasodium {(2-(*R*)-[(4,4-Diphenylcyclohexyl)phosphonooxymethyl]diethylenetetraaminehexaaacetato)(aquo)gadolinium(III)}, 5. Compound **4** (38 mg, 45 μmol) was dissolved in distilled, deionized water (4 mL), and the pH was adjusted to 6.5 with NaOH. The exact ligand concentration of the solution was determined by photometric titration with standardized gadolinium chloride in 0.02 M xylenol orange (pH 4.9, acetate buffer, monitor at 572 nm). There is a marked increase in absorbance once the endpoint has been reached. One equivalent of $GdCl_3$·6H_2O (19.3 mg, 37.5 μmol) was added to the solution of **4** and the pH adjusted to 6.5 by the addition of NaOH to give an aqueous solution of the title compound (1.42 mg of Gd per mL, 9.03 mM). Analytical HPLC showed a single peak (5.9 min with both UV and MS (negative ion, *m/z* = 992 [M − H_2O + H]$^-$) detection.

Preparation of 4.5% (w/v) Human Serum Albumin (HSA) and MS-325/HSA Samples. HSA was dissolved in a buffer (PBS) of 10 mM sodium phosphate and 150 mM sodium chloride (pH 7.4). The protein concentration was determined by measuring its absorbance at 280 nm and comparing the reading to a standard curve constructed from the absorbance of HSA standards with 2, 4, 6, 8, and 10 g/dL, respectively, in PBS buffer. Once the HSA concentration was determined, enough PBS was added to dilute the protein to 4.5 g/dL (i.e., 4.5% w/v).

Two 4.5% (w/v) HSA solutions were made: one containing MS-325 at a concentration of 5.3 mM and one without MS-325. The uncertainty in HSA concentration of these 4.5% (w/v) HSA solutions was estimated to be ±0.045% (w/v). An HSA molecular weight of 66 435 Da was used to convert % (w/v) to a molar concentration.

Ultrafiltration Measurements of Binding of MS-325 to HSA. MS-325/HSA samples ranging from 0.051 to 5.3 mM MS-325 in 4.5% (w/v) HSA were made by combining appropriate amounts of 4.5% (w/v) HSA and 4.5% (w/v) HSA/5.3 mM MS-325.

Aliquots (400 μL) of these samples were placed in 5 kDa ultrafiltration units, incubated at 37 °C for 20 min, and then centrifuged at 3500*g* for 7 min. The filtrates from these ultrafiltration units were used to determine the free concentration of MS-325 of each of the samples. Duplicate aliquots were processed for each concentration sample of MS-325 in 4.5% (w/v) HSA, with the exception of the lowest and highest concentration samples, which were processed seven times.

Drug concentrations of MS-325/HSA samples and ultrafiltrates were determined by measuring the Gd concentration using ICP-MS. Average

relative uncertainties in the ICP-MS Gd concentrations (with a 95% confidence level) of 2.8% and 4.3% were found for the original MS-325/HSA samples and ultrafiltrates, respectively.

Determination of Dissociation Constants for Fluorescent Probes. All fluorescence measurements were performed in a Perkin-Elmer HTS-7000+ fluorescence plate reader. The fluorescence of 2 μM solutions of each of the fluorescent probes (in PBS buffer) was measured while increasing the HSA concentration from 0 to 50 μM. Binding to HSA caused an enhancement of fluorescence of each of the probes. Under the wavelengths chosen, there was no fluorescence due to unbound ligand. The fluorescence background due to HSA was determined by measuring the fluorescence of 0−50 μM HSA (in PBS buffer), without the presence of any fluorescent probe; this background was then subtracted from fluorescence data in the HSA titration into 2 μM fluorophore. The excitation and emission wavelengths used for the dansyl molecules were 360 and 465 nm, respectively (obtained using the standard narrow-band fluorescence filters supplied with the plate reader). The excitation and emission wavelengths used for warfarin were 320 and 380 nm, respectively (filters obtained from Corion Corp., Franklin, MA). The 320 nm filter was rated for fluorescence, with a bandwidth of ±10 nm. The 380 nm filter was rated for absorbance, with a bandwidth of ±6 nm.

The fluorescence data were fit using eq 10, where F represents the

$$F = \frac{P}{2}\{([HSA_t] + [FP_t] + K_d) - \sqrt{([HSA_t] + [FP_t] + K_d)^2 - 4[HSA_t][FP_t]}\} \quad (10)$$

background-corrected fluorescence, $[HSA]_t$ and $[FP]_t$ are the total concentrations of HSA and the fluorescent probe, respectively, K_d is the dissociation constant of the fluorescent probe bound to HSA, and P is the fluorescence of the fluorescent probe bound to HSA per unit concentration. The parameters P and K_d were obtained by fitting the fluorescence data using eq 10 and the program KaleidaGraph (version 3.08, Synergy Software, Reading, PA).

Determination of Site-Specific Binding Dissociation Constants for MS-325. A solution containing [fluorescent probe] ~ [HSA] ~ K_d and 400 μM MS-325 was prepared. Aliquots of this solution were 2-fold diluted serially by addition of a solution which contained the same concentrations of fluorescent probe and HSA but no MS-325. In all, this produced eight samples of different concentrations of MS-325 (differing by a factor of 2), but all containing the same concentration of fluorophore and HSA. The fluorescence of 100 μL aliquots of each of these samples was measured in quadruplicate in 96 well plates. Sixteen 100 μL aliquots of the solution containing no MS-325 (maximum fluorescent intensity) were also measured in the same 96 well plate, along with sixteen 100 μL aliquots of HSA in PBS (minimum fluorescent intensity). These two controls set the dynamic range for fluorescence change when MS-325 displaces a fluorescent probe.

The K_i of MS-325 was determined in the following way. The fractional drop in fluorescence at a particular MS-325 concentration was interpreted as a fractional displacement of the bound fluorescent probe. Since the initial concentration of bound probe was known from its K_d, the observed fluorescence could be converted to a concentration of fluorescent probe bound to HSA, $[FP]_{bound}$. The concentration of bound probe is also given by eq 11, where K_d^{app} is the apparent

$$[FP]_{bound} = \{([HSA]_t + [FP]_t + K_d^{app}) - \sqrt{([HSA]_t + [FP]_t + K_d^{app})^2 - 4[HSA]_t[FP]_t}\}/2 \quad (11)$$

$$K_d^{app} = K_d\left(1 + \frac{[MS-325]_{free}}{K_i}\right) \quad (12)$$

dissociation constant of the probe in the presence of MS-325 and is related to K_d by eq 12. K_i represents the site-specific dissociation constant for MS-325. The $[FP]_{bound}$ measured from fluorescence was compared to the $[FP]_{bound}$ calculated using eqs 11 and 12. Three parameters were iteratively varied using the Solver function of Microsoft Excel 98 (Microsoft, Redmond, WA): K_i, the initial fluorescence (±15%; this represented the scatter in the initial fluorescence and took into account any changes in solution composition upon adding MS-325), and the fluorescence in the absence of the probe, total displacement (±15%). The program varied these three parameters to minimize the sum of the squares of the residuals from measured and calculated $[FP]_{bound}$. The experiment was performed five times with dansyl sarcosine, four times with dansyl-L-asparagine, and twice with warfarin.

Relaxivity. Relaxivities were determined at 20 MHz (0.47 T) and 64.5 MHz (1.5 T) using a Bruker NMS 120 Minispec and a modified Varian XL-300, respectively. T_1 was measured with an inversion recovery pulse sequence, and all samples were measured at 37 °C. The T_1 and T_2 NMRD profiles (37 °C) were recorded on a custom-built relaxometer using saturation transfer and CPMG pulse sequences, respectively.

^{17}O NMR. $H_2{}^{17}O$ chemical shifts and relaxation rates were determined for a PBS buffer solution in the presence and in the absence of 10 mmolal MS-325 as a function of temperature (0−100 °C) on a Varian Unity 300 NMR operating at 40.6 MHz. Probe temperatures were determined from ethylene glycol or methanol chemical shift calibration curves. T_1 was determined by inversion recovery and T_2 by a CPMG pulse sequence.

The program Scientist (ver. 2.0, Micromath, Salt Lake City, UT) was used to fit the relaxation rate data and the binding data to the stoichiometric model.

Acknowledgment. Prof. I. M. Klotz is thanked for an insightful commentary on the binding studies. Drs. J. Ellison and A. Kolodziej are kindly acknowledged for useful discussions. W.D.H. acknowledges NSF Grant CHE-9705788 for partial support. The analytical department at EPIX Medical, Inc., is thanked for numerous ICP determinations.

Supporting Information Available: Analysis of ^{1}H and ^{17}O relaxation rate data; Table S1 listing total, percent bound and unbound concentrations of MS-325, and corresponding ratios of bound MS-325:HSA:free MS-325; Table S2 listing reduced transverse relaxation rates for MS-325 and $[Gd(DTPA)(H_2O)]^{2-}$ as a function of temperature (PDF). This material is available free of charge via the Internet at http://pubs.acs.org.

JA017168K